1 September 2000

ELSEVIER

Optics Communications 183 (2000) 51–63

OPTICS COMMUNICATIONS

www.elsevier.com/locate/optcom

Optimum configuration and design of 1480-nm pumped L-band gain-flattened EDFA using conventional erbium-doped fiber

Tsair-Chun Liang [a,*], Yung-Kuang Chen [b,1], Jing-Hong Su [b], Weng-Hung Tzeng [b], Chiek Hu [c], Ying-Tso Lin [c], Yin-Chieh Lai [c,d]

[a] *Department of Telecommunication Engineering, National Kaohsiung Institute of Marine Technology, Kaohsiung 811, Taiwan*
[b] *Institute of Electro-Optical Engineering, National Sun Yat-Sen University, Kaohsiung 804, Taiwan*
[c] *Opto-Electronics and Systems Lab., Industrial Technology Research Institute, Chutung, Hsinchu 310, Taiwan*
[d] *Institute of Electro-Optical Engineering, National Chiao Tung University, Hsinchu 300, Taiwan*

Received 18 May 2000; accepted 4 June 2000

Abstract

We theoretically investigate optimum configurations of 1480-pumped L-band (1570–1610 nm) gain-flattened erbium-doped fiber amplifier (EDFA), using conventional erbium-doped fiber, for multi-wavelength wavelength division multiplexing (WDM) systems. The design criterion of L-band EDFA is to achieve the highest channel output power while keeping the differential channel output power to be ≤ 0.7 dB among 32 digital baseband channels with low channel noise figure of ≤ 5.5 dB. A total of nine L-band EDFA configurations are examined and compared. These configurations considered include the dual-forward, dual-backward, and different bi-directional pumping schemes, each with and without the midway optical isolator. Among all configurations, we find that the pump-passed case in forward-and-backward pumping scheme is the best amplifier configuration to offer the highest channel output power with good channel gain uniformity and moderate low noise figure. In addition, the tolerance of the ratio of first-staged EDF length to the total EDF length, and the effects of optical isolation of midway isolator, and pump power degradation on the characteristics of the best configuration are also examined. This investigation provides the EDFA configuration selection for multi-wavelength WDM L-band lightwave systems. © 2000 Published by Elsevier Science B.V.

Keywords: Optical amplifier; Erbium-doped fiber amplifier; L-band EDFA; L-band amplifier; Wavelength-division multiplexing; Optical fiber communication

1. Introduction

It is vitally important to increase the number of optical channels in wavelength division multiplexing (WDM) transmission systems. One way to increase channel numbers is to narrow the channel spacing. However, it will worsen the nonlinear effects such as cross-phase modulation (XPM) or four-wave mixing (FWM) [1,2], and makes accurate wavelength control of optical senders necessary. Another way to increase the channel number is to widen the usable wavelength bandwidth in low loss region of the used single-mode fiber.

* Corresponding author. Fax: +886-7-525-4499; e-mail: tcliang@mail.nkimt.edu.tw
[1] E-mail: ykchen@mail.nsysu.edu.tw.

0030-4018/00/$ - see front matter © 2000 Published by Elsevier Science B.V.
PII: S0030-4018(00)00873-7

Erbium-doped fiber amplifiers (EDFAs) have emerged as vital components for optical fiber networks, serving a wide range of applications from WDM network repeaters to cable-television (CATV) power amplifiers and in-line amplifiers. The WDM optical fiber amplifier with a flattened amplification region from 1530- to 1560-nm (conventional band, C-band) has been well investigated [3,4]. Recently, the other new band, the long wavelength region from 1570 to 1610-nm (L-band), has also been widely investigated [5–15] through the use of a long conventional EDF and is very attractive for doubling of the transmission capacity. L-band EDFAs are attractive for application to WDM transmission systems not only as they can increase the amplification wavelength range but they also enable us to construct a WDM transmission system using dispersion-shifted fiber (DSF) without any degradation caused by FWM [16].

The amplification characteristics of L-band EDFAs by single-staged with a single forward pumped in the 980 and 1480-nm bands have been investigated by H. Ono et al. [9]. Owing to the 1550-nm ASE generated by 1480-nm band pumping is the pump source of 1580-nm band amplification and the quantum conversion efficiency to 1550-nm ASE with 1480-nm band pumping is higher than that with 980-nm band pumping, the flattened gain coefficient (flatted signal gain to pump power ratio) with 1480-nm band pumping were more than twice as high as those with 980-nm band pumping. On the other hand, the noise figure with 1480-nm band pumping was only degraded of 0.5 dB by compared with those for 980-nm band pumping. Therefore, the 1480-nm pumping schemes are considered in this work. Several 1480-nm pumped L-band EDFAs have been reported such as the bi-directional forward-and-backward pumping scheme without a midway optical isolator [17], dual-backward pumping scheme [8], single-forward pumping scheme [9], and bi-directional forward-and-backward pumping scheme with a midway isolator [18]. However, the optimum configuration of such 1480-nm pumped L-band EDFA to offer the maximum channel output power with good channel output power uniformity and low noise figure characteristics has not yet been reported.

In this paper, we theoretically investigate and compare various 1480-nm pumping EDFA configurations without using external gain equalization technique to amplify 32 digital WDM channel signals operated in the long-wavelength band of 1570–1610 nm. The design criterion is to keep the differential channel output power to be ≤ 0.7 dB among digital channels with low channel noise figure of ≤ 5.5 dB. These configurations considered include single-stage and two-stage designs in dual-forward, dual-backward, and various bi-directional pumping schemes, each with and without the midway optical isolator. For bi-directional pumping case, the pump-power passed and blocked arrangements are further considered. For the two-stage design, the effects of percentage of first-stage EDF length, and the optical isolation of a midway isolator for the scheme with midway isolator case on the influence of EDFA performance are studied. The effects of pump power and input power of these configurations on EDFA performance are also investigated. A total of nine configurations are examined and compared. The investigation result provides the best L-band EDFA configuration to design both power and in-line amplifiers for multi-wavelength L-band WDM lightwave systems.

The rest of the paper is organized as follows. In Section 2, the amplifier configurations with various pumping schemes are firstly introduced, and then the EDFA modeling and simulation considerations are presented. Section 3 presents the optical channel gain, channel output power, and channel noise figure characteristics for various amplifier configurations in dual-forward, dual-backward, and various bi-directional pumping schemes. The effects of pump power, input signal power, the optical isolation of midway isolator, and the percentage of first-stage EDF length of two-stage amplifier structures on the influence of EDFA performance are also investigated in detail. In Section 4, we present the optical channel gain, chan-

Fig. 1. Various configurations of 1480-nm-pumped L-band EDFA in (a) dual-forward, (b) dual-backward, (c) bi-directional forward and backward, and (d) bi-directional backward and forward pumping schemes.

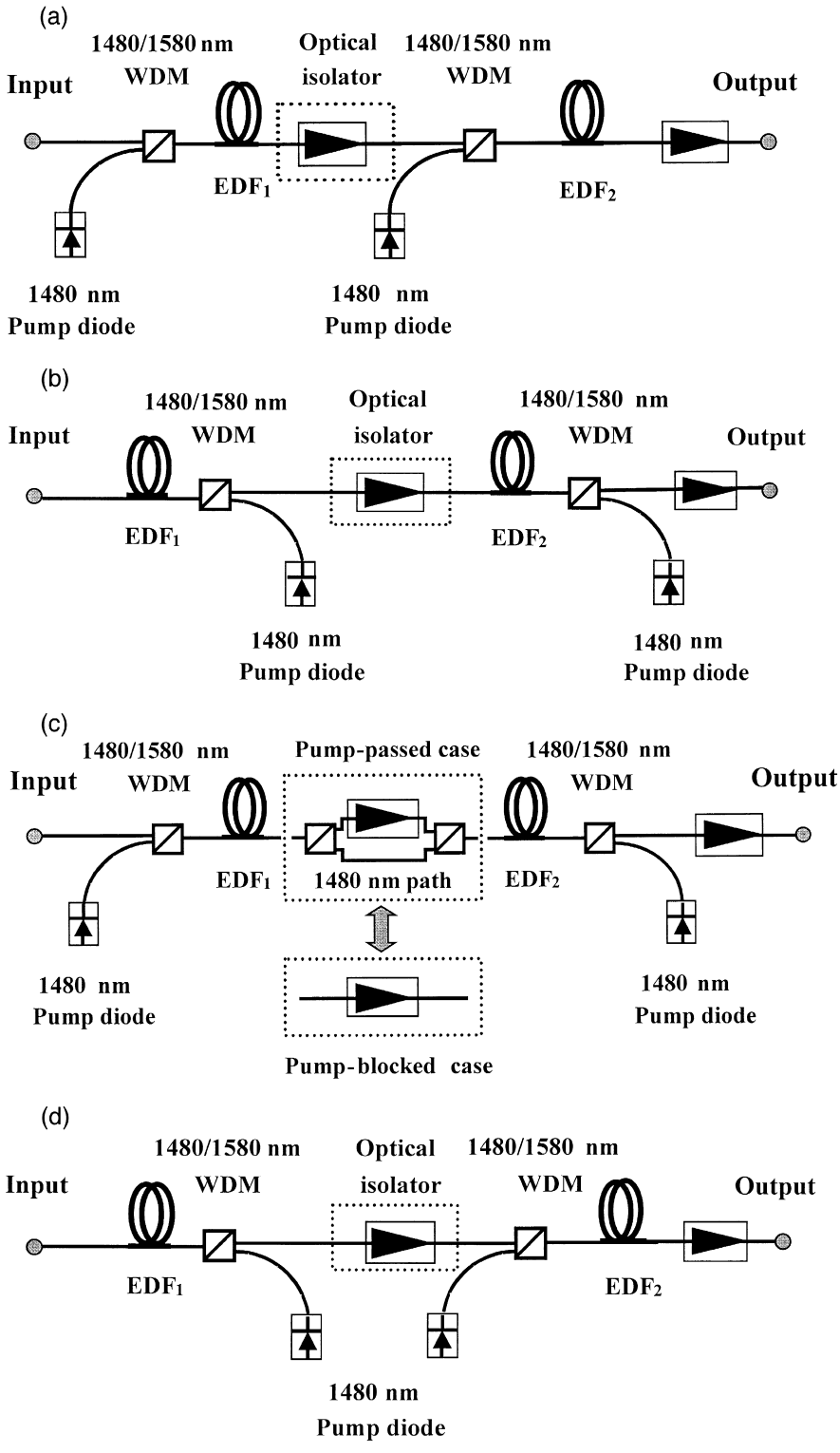
(a)
1480/1580 nm
WDM
Optical
isolator
1480/1580 nm
WDM
Input
Output
EDF1
EDF2
1480 nm
Pump diode
1480 nm
Pump diode
(b)
1480/1580 nm
WDM
Optical
isolator
1480/1580 nm
WDM
Input
Output
EDF1
EDF2
1480 nm
Pump diode
1480 nm
Pump diode
(c)
1480/1580 nm
WDM
Pump-passed case
1480/1580 nm
WDM
Input
Output
EDF1
1480 nm path
EDF2
1480 nm
Pump diode
1480 nm
Pump diode
Pump-blocked case
(d)
1480/1580 nm
WDM
Optical
isolator
1480/1580 nm
WDM
Input
Output
EDF1
EDF2
1480 nm
Pump diode

nel noise figure, and the channel ASE power at different position of EDF, especially for the optimum configuration. Finally, we summarize the paper and present our conclusions in Section 5.

2. L-band EDFA configurations and modeling

Fig. 1 depicts the high-power low-noise L-band EDFA configurations in (a) dual-forward, (b) dual-backward, (c) bi-directional forward-and-backward, and (d) bi-directional backward-and-forward pumping schemes. For each pumping scheme, two pieces of conventional erbium-doped fibers (EDF_1 and EDF_2) and two 1480/1580-nm WDM couples are employed to act as the gain media and the pump/signal combiner, respectively. The dual-forward pumping scheme as shown in Fig. 1(a) is named due to the fact that there are two 1480-nm pump semiconductor LDs used and the propagation direction of the pump lights is the same as the signal light. Similarly, the dual-backward pumping as shown in Fig. 1(b) is named because two pump LDs are used and the propagation direction of the pump lights is opposite to the signal light. The bi-directional forward-and-backward pumping scheme as shown in Fig. 1(c) is named due to two pump laser diodes are used to pump the EDF's from both sides. The bi-directional backward-and-forward pumping scheme as shown in Fig. 1(d) is named due to adopting backward-pumping for the first-stage fiber, EDF_1, and forward-pumping for the second-stage fiber, EDF_2.

Both dual-forward (FF and FFI) and dual-backward (BB and BBI) pumping EDFA's are the two-stage configurations, in which the midway optical isolator acts as an amplified spontaneous emission (ASE) suppression component. The narrowband optical bandpass filter as an ASE suppression component is not considered here due to its inhibition of multi-wavelength WDM operation. The forward-and-backward bidirectional pumped EDFA as shown in Fig. 1(c) is a two-stage configuration when the inter-stage component is used. There are two operation cases for this amplifier structure; one is the pump-passed case (hereafter, FBIp) and another one is the pump-blocked case (hereafter, FBIb). The pump-blocked type as shown in the lower dotted block is the case that when an inter-staged optical isolator is used as the ASE suppressor, in which the forward 1480-nm pump power will be further attenuated by the insertion loss of the midway isolator. On the other hand, the backward 1480-nm pump power will be drastically blocked by the reverse optical isolation of the midway isolator. For the pump-passed case, when a pair of WDM is inserted, the residual pump power is able to pass to the opposite EDF side through the lower 1480-nm path as shown in the upper dotted block. In the mean time, the optical isolator, which is located in the upper optical path, is used to suppress the backward ASE. On the contrary, this two-stage configuration becomes to a single-stage configuration (hereafter, FB) when all inter-staged components are removed. The backward-and-forward bi-directional pumped EDFA as shown in Fig. 1(d) is also a two-stage configuration whether the inter-stage component is used (hereafter, BFI) or not (hereafter, BF). Table 1 lists nine kinds of L-band EDFA configurations and their configuration symbols.

The simulation tool used in this work is the Lucent Technologies OASIX optical amplifier simulation system (Version 2.5), in which the EDFA model used in this work is based on the model by Giles and Desurvire [19]. The conventional EDF characteristics and EDFA parameters used in the simulations are summarized in Tables 2 and 3, respectively. The insertion loss of each WDM coupler is assumed to be the same with 0.5 dB at both 1480 and 1580 nm bands. The isolation of optical isolator is assumed to be 50 dB. The 1480-nm pump output power of each pump laser diode is assumed to be 140 mW. A 32-channel signal in the 1574.54 ~ 1600.60 nm wavelength range with a channel spacing of 0.8 nm is considered. The input signal power level of each digital channel for each EDFA configuration is set to be -15 dBm at 1580 nm region.

There are only two optical connectors used and the others are splicing points for all components within the proposed EDFAs. The insertion loss of each splicing point is assumed to be 0.1 dB. Assume that the optical connectors used at the input and output ports of the L-band EDFA are all angled physical contact (APC) type with low back-reflection of ≤ -60 dB. The return loss of each splicing point and all other optical components used within the

Table 1
Nine kinds of L-band EDFA configurations and their configuration symbols

Midway optical isolator	Pumping schemes	Configuration symbols
Yes	1. dual forward	FFI
Yes	2. dual backward	BBI
Yes	3. bi-directional, forward-backward, pump-blocked	FBIb
Yes	4. bi-directional, forward-backward, pump-passed	FBIp
Yes	5. bi-directional, backward-forward	BBI
No	6. dual forward	FF
No	7. dual backward	BB
No	8. bi-directional, forward-backward	FB
No	9. bi-directional, backward-forward	BF

EDFA is ≤ -60 dB. Therefore, the optical reflection induced performance degradations of bit-error-rate (BER) can be neglected.

3. Characteristic comparison

For investigating the optical gain, and noise figure characteristics of each EDFA configuration, the first step is to find the optimum EDF total length of each amplifier configuration for simultaneously achieving the highest channel output power with differential channel output power ΔP ($\Delta P = P_{max} - P_{min}$) of $\leq$ 0.7 dB among 32 digital channels and the noise figure of ≤ 5.5 dB. Note that the optimum total fiber length here is obtained for maximizing the total output power for the EDFA configuration operated at the input power level of -15 dBm for each digital channel. Fig. 2 shows the required optimal EDF total length and the first-stage gain fiber EDF1 length for various amplifier configurations, where $EDF_{total} = EDF_1 + EDF_2$. In order to obtain the optimum EDF total length, we used two iteration loops to achieve total maximum output power and the noise figure ≤ 5.5 dB for each channel for each amplifier configuration. The range of EDF_1 and EDF_2 lengths set in the simulation are $1 \sim 300$ m; the increment length of each EDF used in two iteration loops is 1 m. We found that the EDF_1 length shorter than the EDF_2 length is required for FBIp, BFI, BF, BBI, and BB amplifier configurations. On the other hand, the EDF_1 length of FFI, FF, and FBIb amplifier configurations is about $76 \sim 79\%$ of the optimum EDF total length. Among these nine configurations, FBIp scheme re-

Table 2
Characteristics of conventional erbium-doped fiber used in this work

Cutoff wavelength	935 nm
Core radius	1.93 μm
Index step (Δn)	0.0117
Numerical aperture	0.185
Mode field diameter	6.7 μm
Background loss @ 1.55 μm	0.72 dB/km
Loss @ 1580 nm	0.4 dB/m
Peak absorption coefficient @ 1.53 μm	4.35 dB/m
Peak absorption coefficient @ 1.48 μm	1.6 dB/m
Erbium concentration	6.5×10^{24} m^{-3}

Table 3
EDFA simulation parameters used in this work

Signal wavelengths	1574.54–1600.6 nm, 32 channels with channel spacing 0.8 nm, separately.
Input signal power	-15 dBm per channel
Pump wavelength	1480 nm
Pump power per pump laser	140 mW
WDM coupler pump loss @ 1480 nm	0.5 dB
WDM coupler signal loss @ 1580 nm	0.5 dB
Insertion loss of optical isolator	0.5 dB
Isolation of optical isolator	50 dB

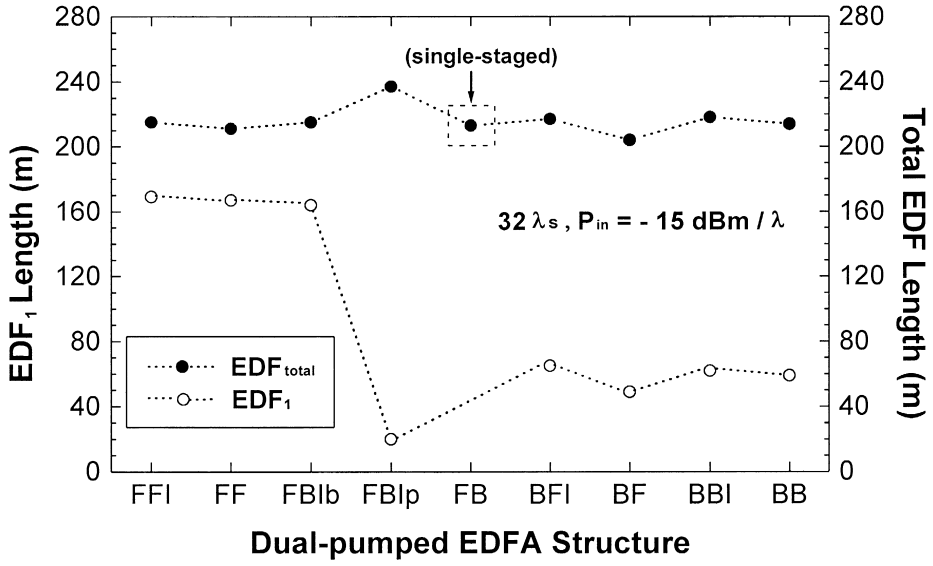

Fig. 2. Optimum EDF total length and the EDF_1 length for various dual-pumped L-band amplifier configurations, operated with the 1480-nm pump output power of 140 mW for each pump laser diode, and 32-channel signals with a channel spacing of 0.8 nm (1574.54 ~ 1600.60 nm) and a channel input power level of −15 dBm.

quires the longest optimal EDF total length of 237 m, and BF scheme required the shortest optimal EDF total length of 204 m.

Fig. 3 shows (a) the channel output power and (b) the spectral noise figure characteristics of four amplifier configurations in the optimum EDF lengths without using midway optical isolator. For these four amplifier schemes without using the midway isolator, the FB scheme has the highest channel output power of about 5.3 mW per channel. The FF scheme has the lowest NF of about ≤ 4.4 dB. On the contrary, the BF configuration exhibits the lowest output power with rather worse noise figure as compared with other configurations. The noise figure characteristics of ≤ 5 dB can be maintained only for FB and FF schemes. Fig. 4 shows (a) the channel output power and (b) the spectral noise figure characteristics of five amplifier configurations with using midway optical isolator operated at the optimum EDF total length condition for the channel input signal of −15 dBm. The low noise figure characteristics of ≤ 5 dB can only be maintained for FBIp, FBIb and FFI pumping schemes. Note that these schemes are all forward pump for the first-stage fiber EDF_1. The noise figure characteristic for the forward pumping scheme is inherently low due to the nearly full population inversion operation of the first-stage EDF in these two-staged L-band amplifiers. Table 4 summarizes the maximum and minimum gains, the maximum and minimum noise figures, the ratios of first-stage EDF to the total EDF length, EDF_1/EDF_{Total}, for these nine EDFA configurations. From the maximum output power with satisfied NF point view, among these nine amplifier configurations, FBIp pumping scheme can get the best channel output power of about 6.1 mW per channel with a moderate noise figure of ≤ 4.7 dB.

4. Characteristics of FBIp configuration

Based on the simulation results listed in Table 4, the FBIp pumping scheme is the best L-band EDFA choice for offering the highest channel output power with good channel gain uniformity and low noise figure characteristics for multi-wavelength L-band WDM lightwave systems. Fig. 5 shows the gain and noise figure characteristics at the end of stage-1 and the output port of FBIp-type EDFA, respectively.

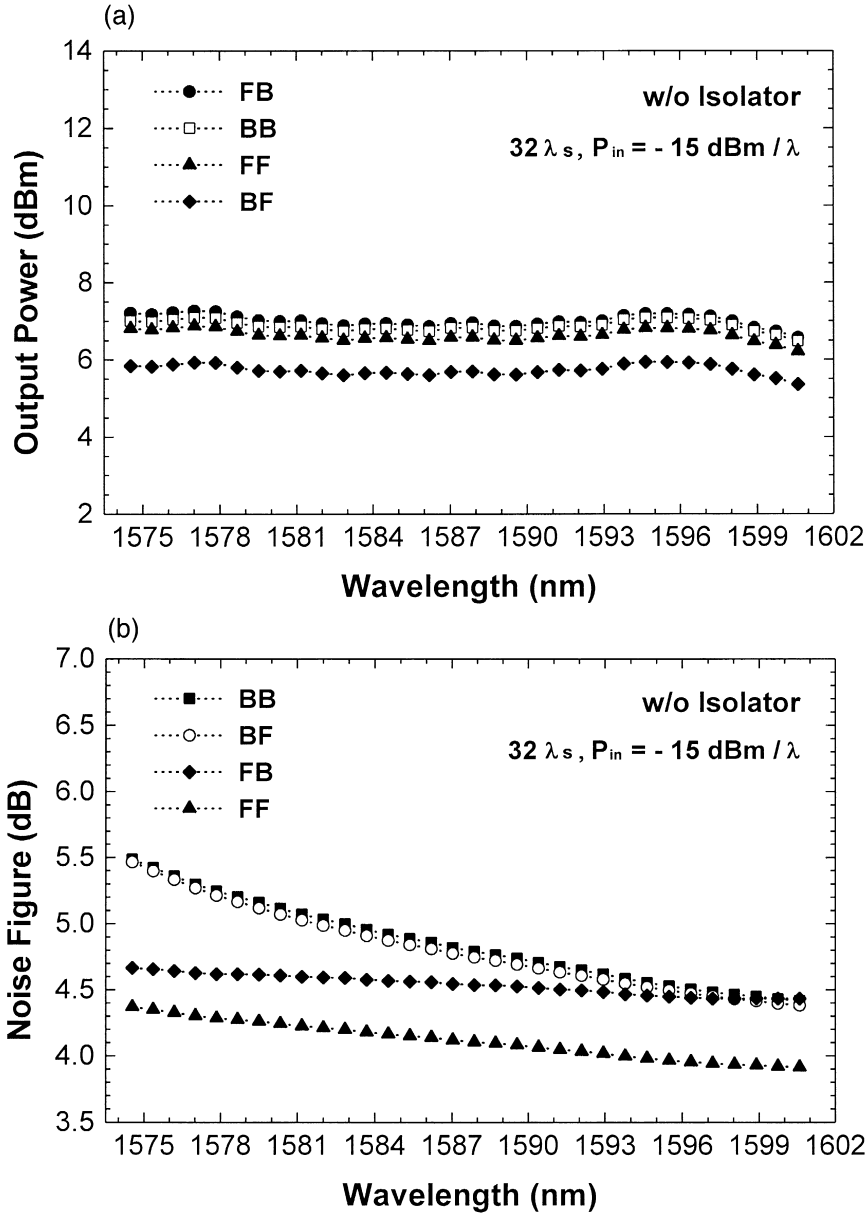

Fig. 3. The characteristics of (a) channel output power and (b) channel noise figure of four amplifier configurations without using the midway optical isolator.

The corresponding noise figure characteristic is 3.6 ~ 2.9 dB for the stage-1 EDFA and 4.3 ~ 4.7 dB for the cascaded EDFA, respectively. The corresponding channel ASE power evolution at $\lambda = 1585.36$ nm in the EDF total length within the FBIp configuration is showed in Fig. 6. The EDF total length is 237 m and the midway isolator is put at the 20 m (the length of stage-1 EDF). Note that the ASE power at the 20-m position has a 3.3-dB drop (from -36.7 dBm to -40 dBm) for the solid line and a 53.3-dB drop

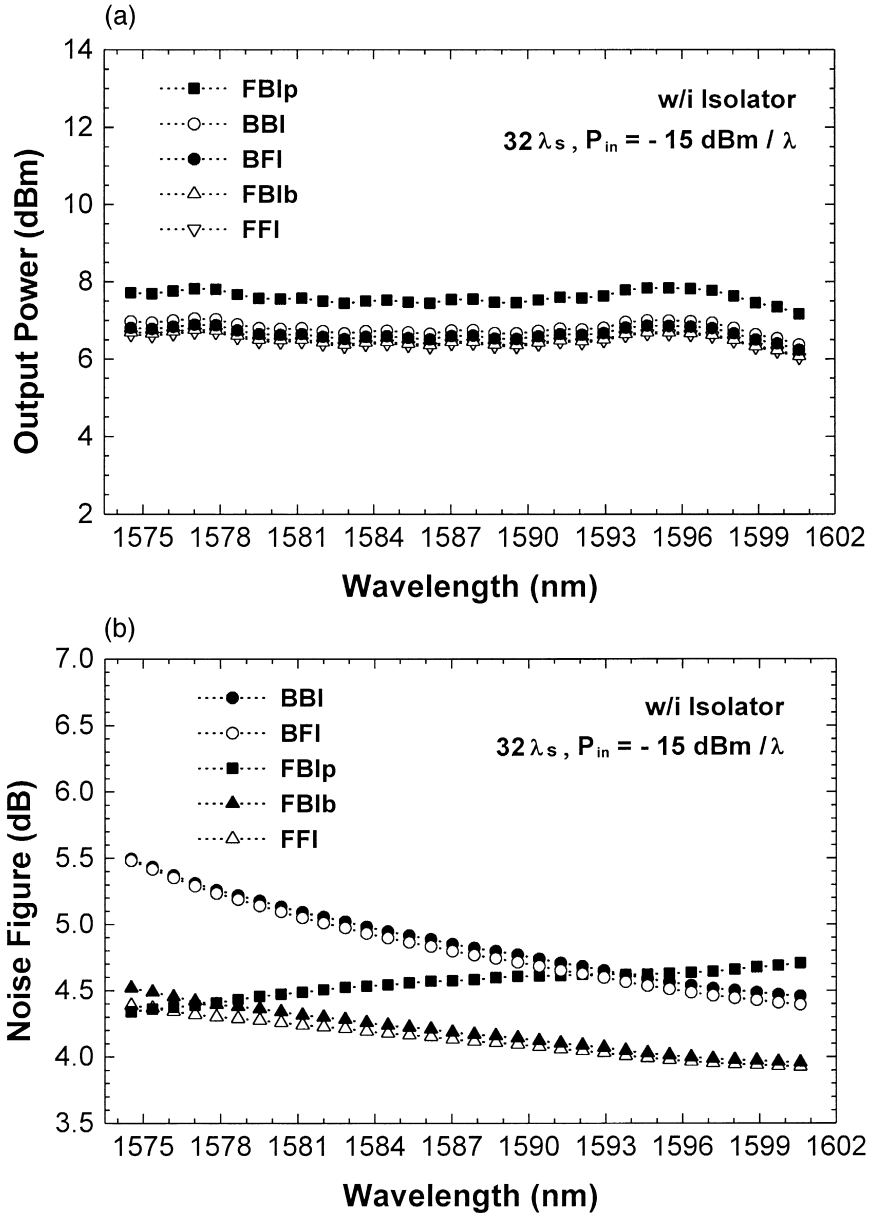

Fig. 4. The characteristics of (a) channel output power and (b) channel noise figure of five amplifier configurations with a midway optical isolator.

(from -21.6 dBm to -74.9 dBm) for the dash line. The results confirm that the insertion loss of inter-staged components including the midway optical isolator is 3.3 dB and the optical isolation of midway optical isolator is about 50 dB.

Fig. 7 shows the maximum gain, the differential channel gain ΔG, and the maximum noise figure characteristics of the FBIp scheme as a function of the ratio of EDF_1 to the total EDF length. When the ratio of EDF_1/EDF_{total} (%) is $\geq 4.6\%$, the noise

Table 4
The inter-stage isolation and the output characteristics of all configurations by optimum EDF total length used in this work

Characteristics[a]	L-band EDFA configurations								
	With midway optical isolator					Without midway optical isolator			
	FFI	FBIb	FBIp	BFI	BBI	FF	FB	BF	BB
Insertion loss of inter-stage (dB)	2.1	2.1	3.3	2.1	2.1	1.5	1.4	1.5	1.5
EDF_1 length (m)	169	164	20	65	62	167	Single-staged	49	59
Optimal EDF total length (m)	215	215	237	217	218	211	213	204	214
EDF_1/EDF_{total} (%)	78.6	76.3	8.4	30.0	28.4	79.1	Single-staged	24	27.6
G_{max} (dB)	21.71	21.76	22.83	21.89	22.04	21.87	22.27	20.94	22.09
G_{min} (dB)	21.04	21.07	22.17	21.24	21.37	21.21	21.57	20.36	21.48
ΔG (dB)	0.67	0.69	0.66	0.65	0.67	0.66	0.70	0.58	0.61
NF_{max} (dB)	4.4	4.5	4.7	5.5	5.5	4.4	4.7	5.5	5.5
NF_{min} (dB)	3.9	4.0	4.3	4.4	4.5	3.9	4.4	4.4	4.4
ΔNF (dB)	0.5	0.5	0.4	1.1	1.0	0.5	0.3	1.1	1.1

[a] Lauched with 32 channel signals, each with an input power level of -15 dBm.

figure achieves ≤ 5.5 dB. On the other hand, the ratio region is within $1.2\% \leq EDF_1/EDF_{total}\ (\%) \leq 16.9\%$, the differential channel gain ΔG of ≤ 0.7 dB is obtained. So, the ratio of $4.6\% \sim 16.9\%$ of EDF_1/EDF_{total}, is the allowable fiber ratio region to meet design criteria of $\Delta G \leq 0.7$ dB and $NF \leq 5$ dB. Fig. 8 shows the effect of input signal power of each channel on the characteristics of maximum gain, the differential channel gain ΔG, and the maximum noise figure of the FBIp configuration. For this FBIp scheme, to maintain the output differential channel gain of $\Delta G \leq 1$ dB and the maximum noise figure of ≤ 5.5 dB for 32 input channels, the allowable input power range is from -15 to -14 dBm. When the channel input power range is from -18 to -11 dBm, the differential channel gain ΔG of ≤ 3 dB

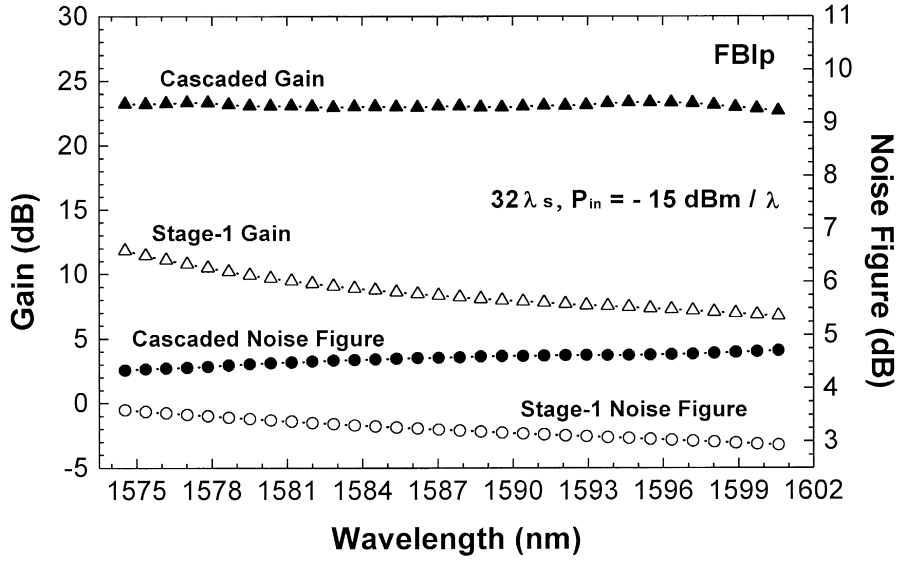

Fig. 5. The evolution of spectral channel gain and noise figure characteristics of the first-staged and the cascaded-staged amplifier for FBIp-type configurations.

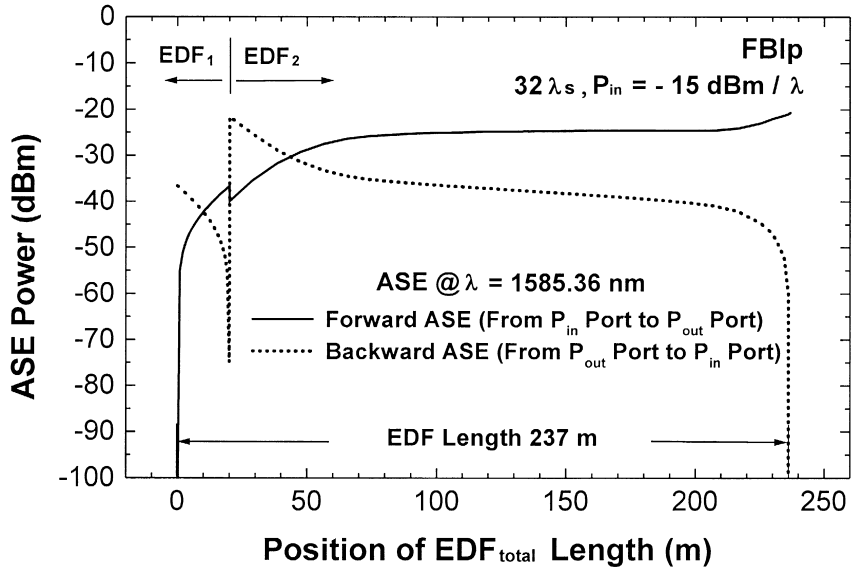

Fig. 6. The forward and backward ASE channel power evolution at $\lambda = 1585.36$ nm for the FBIp configuration versus the position of EDF length.

and the maximum noise figure of ≤ 5.5 dB can be obtained for 32 input channels.

The optical isolation effect of the midway optical isolator on the channel gain and noise figure characteristics of the FBIp configuration is shown in Fig. 9. We find that the channel output power characteristics are independent on the midway isolator when the isolation is greater than and equal to 18 dB. Fig. 10

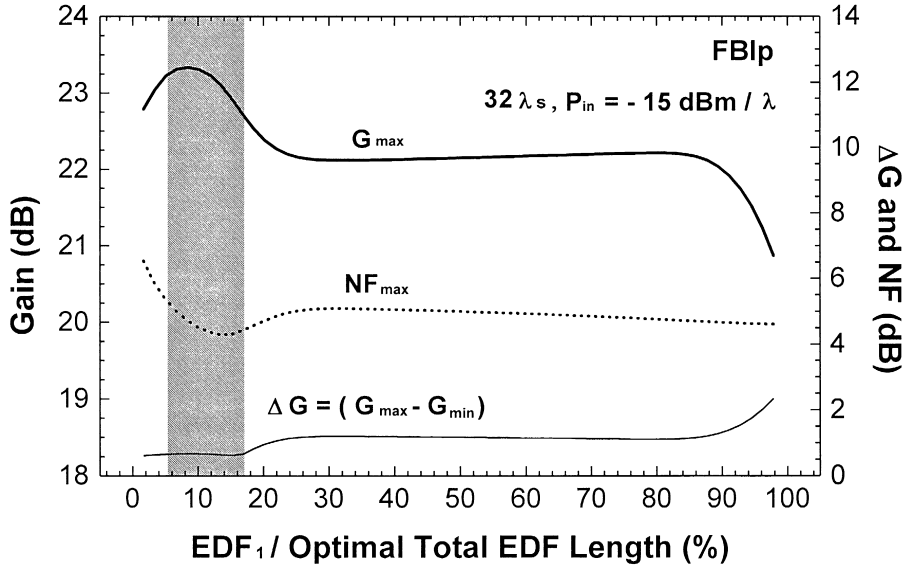

Fig. 7. The effect of EDF_1/EDF_{total} (%) on the differential channel gain ΔG, maximum gain G_{max} and maximum noise figure NF_{max} characteristics of the FBIp-type EDFA.

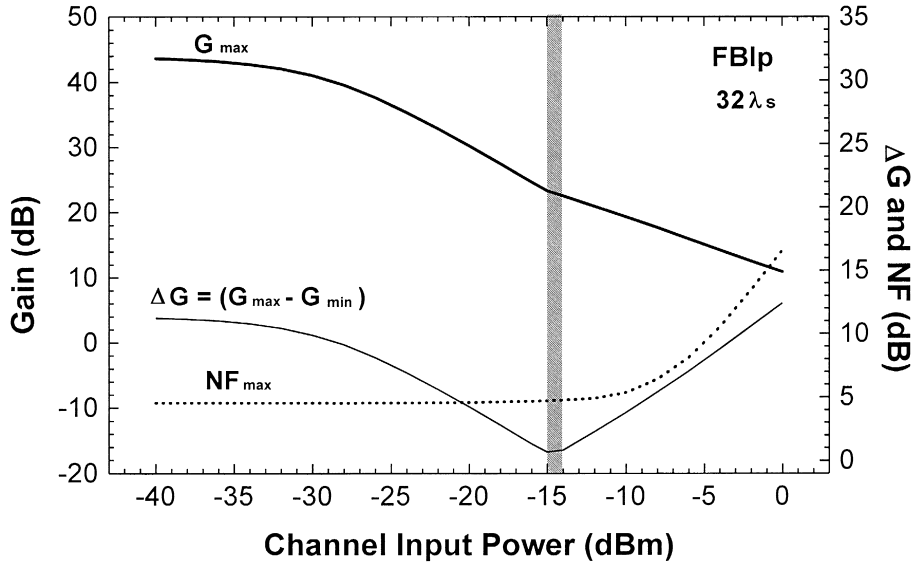

Fig. 8. The effect of input signal power of each channel on the differential channel gain ΔG, maximum gain G_{max}, and maximum noise figure NF_{max} characteristics of the FBIp-type EDFA.

shows the maximum gain, the differential channel gain ΔG, and the maximum noise figure versus the pump power of each laser diode. The maximum channel gain is gradually increasing and the maximum noise figure is gradually decreasing when the pump power of each laser diode is increasing, each

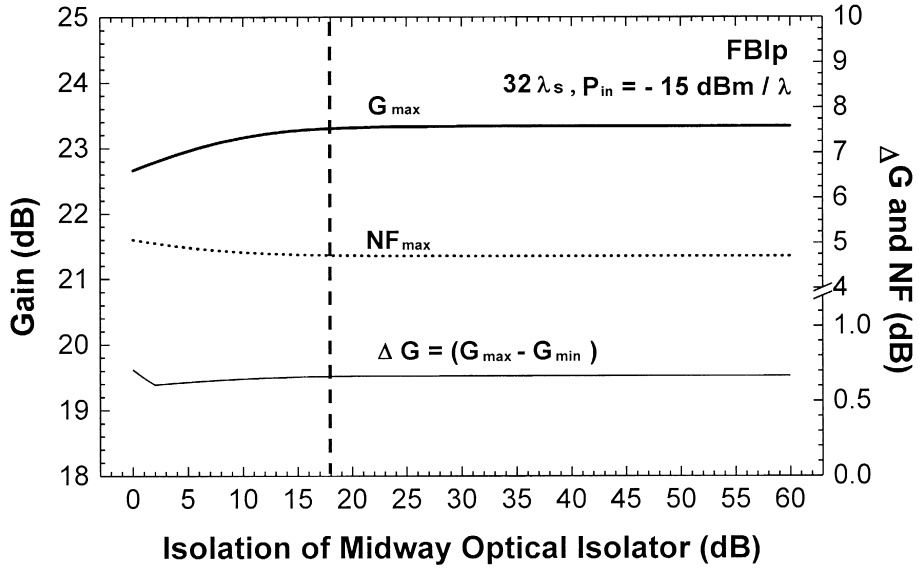

Fig. 9. The effect of optical isolation of midway optical isolator on the differential channel gain ΔG, maximum gain G_{max}, and maximum noise figure NF_{max} characteristics of the FBIp-type EDFA.

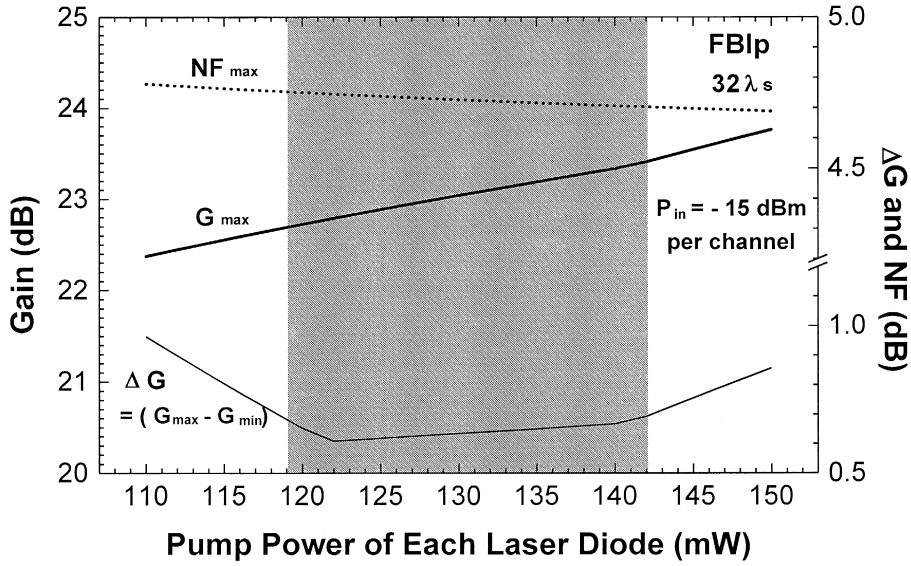

Fig. 10. The effect of pump power degradation of each pump laser diode on the differential channel gain ΔG, maximum gain G_{max}, and maximum noise figure NF_{max} characteristics of the FBIp-type EDFA.

with an input power of −15 dBm per channel. The allowable pump power range of each laser diode is from 119 to 142 mW. That is, it allows a power degradation range of 23 mW of each pump LDs. Fig. 11 illustrates the output spectrum of the FBIp-type EDFA with 32 input signal channels with a channel spacing of 0.8 nm.

In this work we also used a 980-nm pump laser diode to replace with the first pump laser in this FBlp L-band amplifier to investigate the character-

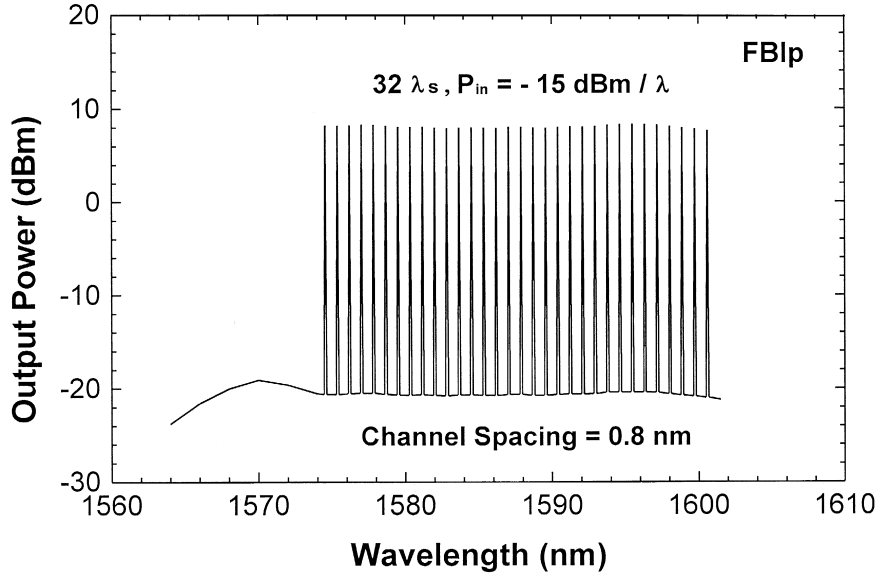

Fig. 11. Calculated optical output spectrum of the FBIp-type EDFA with launched 32 channels, each with −15 dBm input power level.

istics of such 980-nm forward pumped and 1480-nm backward pumped (980-nm + 1480-nm) FBlp scheme. We found that the gain spectrum profile of the 980-nm + 1480-nm pumped FBlp scheme with a 32-channel WDM signals are almost the same as that of the 1480-nm + 1480-nm pumped FBlp scheme, but with a lower channel output power with reduction of about 1 dB, and therefore a reduction of total amplifier output power of about 25 mW, and improved noise figure characteristics of about 0.3 to 0.1 dB. In consequence, from the high channel output with low gain variation of < 0.7 dB and low noise figure of < 5 dB point of view, the 1480-nm + 1480-nm pumped FBlp scheme is better than the 980-nm + 1480-nm pumped FBlp scheme.

5. Conclusions

We have theoretically investigated various configurations of 1480-nm pumped L-band EDFA to simultaneously achieve high gain (≥ 20 dB) with low differential channel gain of $\Delta G \leq 0.7$ dB and low noise figure of ≤ 5.5 dB. A total of nine L-band EDFA configurations using conventional EDF, operated at 32 digital channels with -15 dBm input power per channel, have been examined and compared. Among these configurations, it is found that the pump-passed case in forward-and- backward pumping scheme, FBIp, is the best amplifier configuration to offer the highest output power and gain ($G_{max} = 22.83$ dB, $G_{min} = 22.17$ dB) with moderate low noise figure ($NF_{max} = 4.7$ dB). The isolation of midway isolator of ≥ 18 dB is satisfied for the FBIp-type configuration. Another advantage is that this scheme allows a large fiber length ratio range of 4.6% ~ 16.9% of EDF_1/EDF_{total}, which relaxes the construction of L-band EDFA. In addition, the pump power degradation of up to 23 mW is allowed for this configuration to maintain the characteristics of $\Delta G \leq 0.7$ dB and NF ≤ 4.8 dB, but at the expense of about 0.6 dB degradation of channel gain. Among these configurations, the single-staged forward-and-backward pumping scheme, FB, without using any inter-staged component can offer the second high output power and gain ($G_{max} = 22.27$ dB, $G_{min} = 21.57$ dB) with moderate low noise figure ($NF_{max} = 4.7$ dB). The investigation result provides the L-band EDFA configuration selection for multi-wavelength WDM lightwave systems.

Acknowledgements

This work was supported by the Opto-Electronics and Systems Lab., Industrial Technology Research Institute, Chutung, Hsinchu 310, of Taiwan.

References

[1] D. Marcuse, A.R. Chraplyvy, R.W. Tkach, IEEE/OSA J. Lightware Technol. 12 (1994) 885.
[2] N. Shibata, R.P. Braun, R.G. Waarts, IEEE J. Quantum Electron. QE-23 (1987) 1205.
[3] E. Desurvire, Erbium-Doped Fiber Amplifiers: Principles and Applications, John Wiley and Sons, New York, 1994.
[4] A. Bjarklev, Optical Fiber Amplifiers: Design and System Applications, Artech House, Boston and London, 1994.
[5] J.F. Massicott, J.R. Armitage, R. Wyatt, B.J. Ainslie, S.P. Craigryan, Electron. Lett. 26 (1990) 1645.
[6] J.F. Massicott, R. Wyatt, B.J. Ainslie, Electron. Lett. 28 (1992) 1924.
[7] H. Ono, M. Yamada, Y. Ohishi, IEEE Photon. Technol. Lett. 9 (1997) 596.
[8] H. Ono, M. Yamada, T. Kanamori, S. Sudo, Y. Ohishi, Electron. Lett. 33 (1997) 710.
[9] H. Ono, M. Yamada, S. Sudo, Y. Ohishi, Electron. Lett. 33 (1997) 876.
[10] H. Ono, M. Yamada, T. Kanamori, Y. Ohishi, Electron. Lett. 33 (1997) 1477.
[11] H. Ono, M. Yamada, M. Shimizu, Y. Ohishi, Electron. Lett. 34 (1998) 1509.
[12] H. Ono, M. Yamada, T. Kanamori, S. Sudo, Y. Ohishi, J. Lightwave Technol. 17 (1999) 490.
[13] K.I. Suzuki, H. Masuda, S. Kawai, K. Aida, K. Nakagawa, Electron. Lett. 33 (1997) 1967.
[14] T. Sakamoto, J. Kani, M. Jinno, S. Aisawa, M. Fukui, M. Yamada, K. Oguchi, Electron. Lett. 34 (1998) 392.
[15] H.S. Chung, M.S. Lee, D. Lee, N. Park, D.J. DiGiovanni, Electron. Lett. 35 (1999) 1099.
[16] M. Jinno, T. Sakamoto, J. Kani, S. Aisawa, K. Oda, M. Fukui, H. Ono, K. Oguchi, Electron. Lett. 33 (1997) 882.
[17] H. Ono, M. Yamada, M. Shimizu, Y. Ohishi, Electron. Lett. 34 (1998) 1513.
[18] T. Sakamoto, K. Hattori, J. Kani, M. Fukutoku, M. Fukui, M. Jinno, K. Oguchi, Electron. Lett. 34 (1998) 1959.
[19] C.R. Giles, E. Desurvire, J. Lightwave Technol. 9 (1991) 271.